A COMBINED SHAPE TRACKING AND SPECKLE TRACKING APPROACH FOR 4D DEFORMATION ANALYSIS IN ECHOCARDIOGRAPHY

Colin B. Compas[1], Emily Y. Wong[5], Xiaojie Huang[2], Smita Sampath[3], Ben A. Lin[4], Xenophon Papademetris[1,3], Karl Thiele[6], Donald P. Dione[4], Albert J. Sinusas[4], Mathew O'Donnell[5], James S. Duncan[1,2,3]

Departments of [1]Biomedical Engineering, [2]Electrical Engineering, [3]Diagnostic Radiology, [4]Internal Medicine, Yale University, New Haven, CT USA
[5]Department of Bioengineering, University of Washington, Seattle, WA USA
[6]Philips Medical Systems, Andover, MA USA

ABSTRACT

Quantitative analysis of left ventricular function provides valuable information about overall heart health. Echocardiography is non-invasive method for imaging the heart that provides high temporal resolution allowing for imaging cardiac motion. Shape tracking and speckle tracking are two methods that have previously been used to track cardiac deformation in ultrasound. These two methods provide complementary displacement values. Shape tracking gives accurate boundary displacements, while speckle tracking provides accurate displacements across the myocardium. We combine these two methods using adaptive multilevel radial basis functions on 4D echocardiography data. Radial strains were calculated for N=5 open chest canines 6 weeks post-coronary artery occlusion. Radial strain values for three myocardial segments across three short axis slices showed good correlation to corresponding MR tagged data.

Index Terms— Echocardiography, 4D Ultrasound, Cardiac Strain, Motion Tracking, Radial Basis Functions

1. INTRODUCTION

Quantitative analysis of left ventricular (LV) function is essential for understanding the overall health of the heart. In order to obtain quantitative information about cardiac motion, accurate tracking techniques are required. Accurately tracking cardiac deformation allows for an understanding of both myocardial injury and treatment response. Echocardiography has been a popular method for observing LV deformation due to its high temporal resolution, which allows for imaging of cardiac motion in real time. Echocardiography does not use any ionizing radiation, is portable, and is relatively low cost compared to other methods used for cardiac imaging. The safety and portability of ultrasound (US) means that a critically ill patient can be imaged at bed side over a series of imaging sessions in order to observe changes in cardiac function. US does not rely on a magnetic field to create images, so patients with an implanted pacemaker or defibrillator are still able to be imaged.

Two techniques that have been used to track motion in US images are shape tracking and speckle tracking. Shape tracking methods track a set of points on the surface of the myocardium between image frames and then use an interpolation technique or model to calculate a dense displacement field over the entire myocardium [1]. These feature points can be generated from an image segmentation or directly from image intensity values. The feature points can have a position as well as a feature value, such as curvature, that is used in the matching. The drawbacks to shape tracking methods are that consistent feature points can be difficult to find and that they must rely heavily on models to calculate a final displacement field from the sparse set of points.

Speckle tracking is an alternative approach to motion tracking in US [2]. Speckle is created by the constructive and destructive interference patterns of the back scattering waves and can be used to track motion. A speckle pattern results as the accumulation of the random scatterings from within the tissue being imaged and remains consistent for short time intervals. As a result, it is possible to track this pattern between adjacent image frames. This method gives good displacement values across the myocardium where the signal is consistent, but cannot track on tissue boundaries due to inhomogeneities in the signal.

The nature of these two tracking methods causes them to be complimentary sources of information. Shape tracking provides displacement information on the boundaries of the myocardium, while speckle tracking provides displacements across the myocardium. We have shown that in 2D combining these two methods can distinguish between normal and infarcted tissue [3], the two methods show good correlation with magnetic resonance (MR) tagged data [4], and combining the two methods yields better correlations to MR than ei-

This work was supported by NIH Grant 5R01HL082640-04.

ther method individually [5]. The previous methods were performed on 2D and 2D+t data. We now extend these methods to 4D (3D+t) echocardiography (4DE) data for a complete picture of myocardial deformation. We use 3D radial basis functions (RBFs) to combine the shape tracking and speckle tracking displacements and calculate a dense displacement field over the entire myocardium, . From the displacements we calculate strain values that can be used to assess cardiac function and compare these strains to values generated from MR tagging for validation.

2. METHODS

2.1. Shape Tracking Methods

A brief description of the shape tracking methods used in this work is provided here. For a more detailed description of the algorithm, see [1]. The first step in the shape tracking procedure is image segmentation. We segment 4DE sequences using a sparse-representation-based method introduced in [6]. It exploits the inherent spatio-temporal coherence of tissue/blood appearance for segmenting both endocardial and epicardial boundaries of left ventricle from echocardiographic sequences. The method employs sparse representation of local image appearance. In spatial domain, it models intra-class appearance coherence and interclass appearance difference with series of appearance dictionaries. The appearance dictionaries are trained in a boosting framework to be both reconstructive and discriminative. In temporal domain, it predicts the appearance of the current frame based on the appearance observed in the preceding frames, which results in an appearance discriminant for the current frame. The appearance discriminant is integrated into a region-based level set segmentation process on the basis of Bayesian framework.

Once we have a segmentation for all of the frames in the image sequence we track the motion by following a local surface between adjacent frames. The local surface patches are matched between frames using a shape similarity metric, which minimizes the difference in principal curvatures of the surface patches. For each point on the surface an energy function, which is the difference in principal curvatures, is minimized over a search window on the deformed surface. The magnitude of this energy function gives a quality measure of the point match. At the completion of the shape tracking algorithm we have a set of sparse feature points with three-dimensional displacement vectors.

2.2. Speckle Tracking Methods

Here we present a brief description of the speckle tracking procedure that was performed. For a more detailed explanation of the procedure, see [7]. A 3-D correlation-based speckle tracking algorithm was used to estimate three component tissue motion (axial, azimuthal, and zenithal) using phase-sensitive cross-correlation of the complex analytic representation of the volumetric US RF data. At each pixel in the volume, a 3-D kernel spanning one speckle (0.22 mm x 2.8° x 2.8° (axial azimuthal zenithal)) was used to calculate the normalized, complex cross-correlation coefficient between two successive volumetric frames. The resultant function was filtered with a 3-D Hanning window (approximately 0.55 mm x 2.2° x 2.2° (axial azimuthal zenithal)) and fitted using a parabolic function to locate the subpixel peak position. The axial displacement was further refined using the phase zero crossing of the correlation around the peak estimation.

2.3. Combined Methods

To combine the two methods we use RBFs. RBFs have been used extensively in scattered data approximation [8], as well as in medical imaging for modeling the deformation field in image registration [9] and motion tracking [10, 11]. A major advantage of RBFs is that the function centers can be placed anywhere in the image domain and do not require the complex meshing step necessary in other modeling strategies [12]. These methods follow closely to the methods we presented in [5], but have been extended from two-dimensions to three.

To combine the shape and speckle tracking data we use compactly supported radial basis functions (CS-RBFs) in an adaptive multi-level fashion. RBFs were used because of their ability to handle complex and incomplete geometries. With our focus on the infarct region in the heart our US scans often do not contain the full myocardium. This causes problems when trying to overlay a control point mesh using free form deformation, but can be handled properly by RBFs. CS-RBFs use only local information to calculate a displacement value at a given point. This provides both a computational and practical advantage when calculating the overall displacement field. Due to the periodic nature of cardiac motion, we are able to incorporate displacement information from neighboring frames to calculate each displacement field.

For data at nodes $\mathbf{x_1}$,...,$\mathbf{x_N}$, the general form of an RBF approximation is

$$\mathbf{U}_{dense} = \sum_{i=1}^{N} \lambda_i \phi \left(||\mathbf{x} - \mathbf{p}_i|| \right) \tag{1}$$

where $||\cdot||$ denotes the Euclidean distance between two points, $\mathbf{p}$ are the RBF centers, and $\phi(r)$ is defined for $r \geq 0$. This equation is guaranteed to be solvable for many choices of ϕ. The center points can be placed at any location within the image space, which is advantageous for modeling our complex geometries. The specific ϕ used in this work is one of Wu's compactly supported positive definite RBFs:

$$\phi_s(x) = \phi\left(\frac{||x||}{s}\right), x \in \mathbb{R}^d \tag{2}$$

$$\phi(r) = (1-r)_+^4 \left(3r^3 + 12r^2 + 16r + 4\right) \text{ for r} \geq 0 \tag{3}$$

where $(1-r)_+ = \max(1-r, 0)$, and s is the region of support for the basis function. This function was selected because it exhibits C^2 continuity and the function ϕ is guaranteed to be positive definite for dimensions up to three [8]. The continuity property is important because derivatives of the displacement field must be taken in order to calculate strain values.

The center points for the CS-RBFs are evenly distributed within the myocardium in three dimensions. For each center point there will be a set of displacements from shape tracking and speckle tracking that lie within the region of influence for that center. The region of influence extends not both spatially and temporally. To calculate the displacement field for image frame $\mathbf{I}(t)$, information from the neighboring frames is used, with the influence decreasing with time. The displacement values within the region of influence for a given center are found as a weighted sum of speckle and shape tracking values. These displacements are used to solve for the λ values in Equation 1. The influence of the two methods for a given center is determined by the number of displacement values within the region of influence, as well as the confidence in those displacements.

This algorithm calculates the final deformation field iteratively across multiple levels of basis functions. At each level, the number of RBF centers is increased while the region of influence of each center is decreased. The algorithm is initialized with a few centers with a large region of support. These large scale functions capture the larger motion trends of the heart. As the algorithm proceeds, the smaller scale functions capture finner details of the deformation. This is important in areas of the myocardium that are on the boundary of the injured tissue. The motion pattern of the injured tissue may be different from neighboring tissue that is less affected and it is important to be able to capture these differences. The final deformation field can then be computed as a combination of the deformation fields at each level.

This algorithm takes an adaptive approach to center spacing by determining if a region of the heart needs to be modeled at a finer level of detail using smaller scale functions. Regions that need to be modeled by smaller scale functions are characterized by having high confidence and high variance in the displacement values. If a region exhibits low confidence and high variance this region is likely noisy and we want to smooth it out with larger scale functions. For each center, the variance of the displacements and a mean confidence are calculated in order to determine if it needs to be sub-sampled at higher levels of the algorithm.

3. RESULTS

Three-dimensional cardiac US images were acquired at 40 Hz frame rate using a modified Philips iE33 (Philips Medical Systems, Andover, MA) system with an X7-2 phased array transducer. The probe was suspended in a water bath over the heart for five anesthetized, open-chested canines. The canines were imaged six weeks after surgical occlusion of the left anterior descending coronary artery. All studies were performed with approval of the Institutional Animal Care and Use Committee. RF and B-mode US data were exported for speckle and shape tracking, respectively. Tagged MR imaging was performed for the same five animals on a 1.5T Sonata MR scanner (Siemens Medical Solutions, Erlangen, Germany) using a 1-1 SPAMM pulse sequence [13] and a harmonic phase (HARP) MR software analysis package to compute radial strains [14].

	Anteroseptal	Anterior	Anterolateral
Basal	0.943	0.825	0.821
Mid	0.890	0.872	0.779
Apical	0.771	0.568	0.556

Table 1. Correlation values between the combined US radial strains and the MR tagged radial strains for the three segments of the myocardium around the suspected infarct region across three slices for N=5 canines.

Deformation fields were calculated from end-diastole (ED) to end-systole (ES) using the methods outlined in Section 2.3. The endocardium and epicardium were manually traced in the end diastolic frame in order to initialize the segmentation procedure. This is the only manual interaction necessary for the procedure. Individual frame to frame displacements were accumulated between ED and ES and radial strains were calculated in the regions myocardium affected by the coronary artery occlusion. The sparse input displacements from shape tracking and speckle tracking are shown in Figure 1A. Figure 1B shows the three-dimensional strain map overlaid on the B-mode image, with the infarct region identified. The corresponding radial strain map generated by the MR tagging methods is shown in Figure 1C showing the infarct in the same region of the myocardium. Radial strains were calculated using a heart centric coordinate system.

Table 1 shows the correlation values between radial stain values from the combined approach outlined in Section 2.3 and the MR tagged values for three segments corresponding to the diagram in Figure 1C for three short axis slices. Each correlation value was computed by comparing MR tag and 4DE-derived radial strain values at 8 time points between ED and ES in the same anatomical segment for all N=5 dogs. Segments were determined using anatomical landmarks in each modality. The regions analyzed correspond to those surrounding the suspected infarct region. This region was selected because going forward we want to quantify the changes in myocardial motion as a result of treatment for ischemic injury. We see good correlation between our method and the MR tagging across all the regions of analysis in seven of the nine segments. As can be seen, there are two segments with lower correlation (Apical Ant. and Apical AL). These regions are near the suspected infarct in a number of animals. This causes these regions have less deformation and are therefore more susceptible to errors when calculating strain.

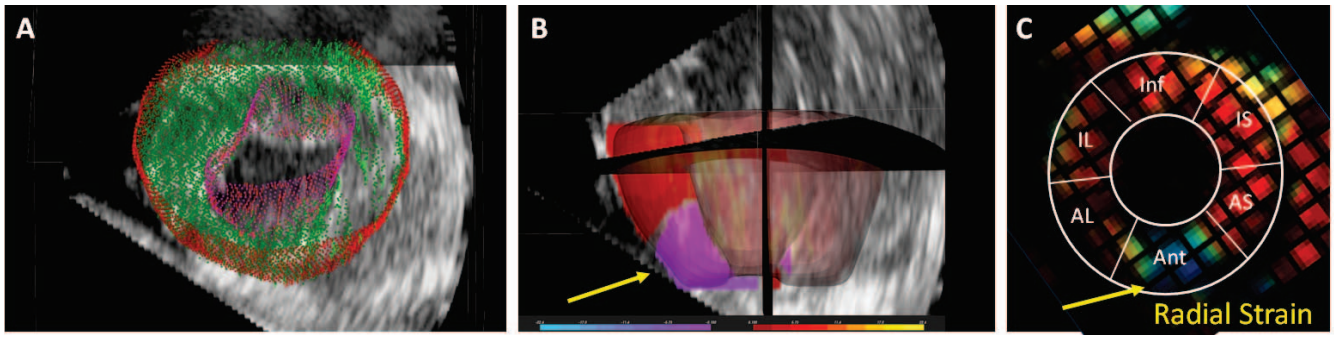


Fig. 1. A) Sparse input vectors with shape tracking (red: epicardial, purple: endocardial), and speckle tracking (green). B) Corresponding dense 3D myocardial radial strain map showing red (positive) normal thickening and purple (negative) in the infarct area near peak systole. C) MR tagging radial strain for the same slice with 6 sectors overlaid.

4. CONCLUSION

We have presented a method for combining shape tracking and speckle tracking displacements for improved deformation analysis of 4DE data. These methods extend upon our previous work with 2D US data and give a more complete picture of LV deformation. Our methods use three-dimensional compactly supported RBFs in an adaptive fashion to combine the two tracking methods. We have shown that our method shows good correlation to radial strain values calculated from MR tagged data. Future directions for this work include applying these methods to close chested canines for analysis of myocardial recovery after occlusion across multiple time points.

5. REFERENCES

[1] P. Shi, A. J. Sinusas, R. T. Constable, E. Ritman, and J. S. Duncan, "Point-tracked quantitative analysis of left ventricular surface motion from 3-D image sequences.," *IEEE Transactions on Medical Imaging*, vol. 19, no. 1, pp. 36–50, Jan. 2000.

[2] X. Chen, H. Xie, R. Erkamp, K. Kim, C. Jia, J.M. Rubin, and M. ODonnell, "3-d correlation-based speckle tracking," *Ultrasonic Imaging*, vol. 27, pp. 21–36, 2005.

[3] C.B. Compas, B.A. Lin, S. Sampath, A.J. Sinusas, and J.S. Duncan, "Combining shape and speckle tracking for deformation analysis in echocardiography using radial basis functions," in *Biomedical Imaging: From Nano to Macro, 2011 IEEE International Symposium on*, 30 2011-april 2 2011, pp. 1322 –1325.

[4] Colin Compas, Ben Lin, Smita Sampath, Congxian Jia, Qifeng Wei, Albert Sinusas, and James Duncan, "Multi-frame radial basis functions to combine shape and speckle tracking for cardiac deformation analysis in echocardiography," in *Functional Imaging and Modeling of the Heart*, vol. 6666 of *Lecture Notes in Computer Science*, pp. 113–120. Springer Berlin / Heidelberg, 2011.

[5] C.B. Compas, B.A. Lin, S. Sampath, Lingyun Huang, Qifeng Wei, A.J. Sinusas, and J.S. Duncan, "Comparing shape tracking, speckle tracking, and a combined method for deformation analysis in echocardiography," in *Healthcare Informatics, Imaging and Systems Biology (HISB), 2011 First IEEE International Conference on*, july 2011, pp. 120 –125.

[6] X. Huang, B.A. Lin, C.B. Compas, A.J. Sinusas, L.H. Staib, and J.S. Duncan, "Segmentation of left ventricles from echocardiographic sequences via sparse appearance representation," *Mathematical Methods in Biomedical Image Analysis*, 2012.

[7] C. Jia, P. Yan, A.J. Sinusas, D. P. Dione, B.A. Lin, Q. Wei, K. Thiele, J. Theodore, J.M. Rubin, L. Huang, J.S. Duncan, and M. Donnell, O'Donnell, "3D elasticity imaging using principal stretches on an open-chest dog heart," *Proceedings of the 2010 IEEE Ultrasonics Symposium*, vol. c, pp. 583–586, 2010.

[8] R. Schaback, "Creating surfaces from scattered data using radial basis functions," *Mathematical Methods for Curves and Surfaces*, pp. 477–496, 1995.

[9] G.K. Rohde, A. Aldroubi, and B.M. Dawant, "The adaptive bases algorithm for intensity-based nonrigid image registration.," *IEEE Transactions on Medical Imaging*, vol. 22, no. 11, pp. 1470–9, Nov. 2003.

[10] Q. Duan, S. Herz, C. Ingrassia, K. Costa, J. Holmes, A. Laine, E. Angelini, O. Gerard, and S. Homma, "Dynamic cardiac information from optical flow using four dimensional ultrasound.," vol. 4, pp. 4465–8, Jan. 2005.

[11] A. Bistoquet, J. Oshinski, and O. Skrinjar, "Myocardial deformation recovery from cine MRI using a nearly incompressible biventricular model.," *Medical Image Analysis*, vol. 12, no. 1, pp. 69–85, Feb. 2008.

[12] P. Yan, N. Lin, A.J. Sinusas, and J.S. Duncan, "A boundary element-based approach to analysis of lv deformation," *International Conference on Medical Image Computing and Computer-Assisted Intervention*, vol. 8, no. Pt 1, pp. 778–85, Jan. 2005.

[13] A.A. Young, C.N. Chang, and L. Axel, "Two-dimensional left ventricular deformation during systole using magnetic resonance imaging with spatial modulation of magnetization.," *Circulation*, vol. 89, no. 2, pp. 740–52, Feb. 1994.

[14] N.F. Osman and J.L. Prince, "Visualizing myocardial function using HARP MRI.," *Physics in Medicine and Biology*, vol. 45, no. 6, pp. 1665–82, June 2000.